$^1_1H^+$- and $^4_2He^+$-induced M-shell x-ray-production cross sections for selected elements in the rare-earth region

R. Mehta, J. L. Duggan, J. L. Price, P. M. Kocur, and F. D. McDaniel
Department of Physics, North Texas State University, Denton, Texas 76203

G. Lapicki
Department of Physics, East Carolina University, Greenville, North Carolina 27834
(Received 1 July 1983; revised 17 October 1983)

The measurements of M-shell x-ray-production cross sections induced by $^1_1H^+$ and $^4_2He^+$ ions are compared to the first-Born-approximation and ECPSSR (energy loss, Coulomb-deflection effects; perturbed-stationary-state approximation, with relativistic corrections) theories. Most of the reported experimental data were measured in our laboratory and the other measurements were taken from the literature. The data from our laboratory were for incident H^+ and He^+ ions in the energy range from 0.25 to 2.5 MeV. The M-shell x-ray-production cross sections were measured for the following thin targets: $_{59}$Pr, $_{60}$Nd, $_{63}$Eu, $_{64}$Gd, $_{66}$Dy, $_{67}$Ho, $_{68}$Er, $_{70}$Yb, and $_{72}$Hf. The data from the literature were for protons and He^+ ions in the energy range from 30 keV to 40 MeV. These data were for the following elements: $_{54}$Xe, $_{59}$Pr, $_{60}$Nd, $_{62}$Sm, $_{63}$Eu, $_{64}$Gd, $_{65}$Tb, $_{66}$Dy, $_{67}$Ho, $_{68}$Er, $_{70}$Yb, $_{72}$Hf, $_{73}$Ta, $_{74}$W, $_{78}$Pt, $_{79}$Au, $_{80}$Hg, $_{82}$Pb, $_{83}$Bi, and $_{92}$U. The first-Born-approximation calculations of the ionization cross section were made using the plane-wave Born approximation for direct ionization and the Oppenheimer-Brinkman-Kramers approximation of Nikolaev for electron capture. The ECPSSR theory of Brandt and Lapicki [Phys. Rev. A 23, 1717 (1981)] goes beyond the first Born approximation and accounts for the energy loss, Coulomb deflection, and relativistic effects in the perturbed-stationary-state theory. The first Born approximation overpredicts all measurements. The ECPSSR theory predicts the M-shell production cross sections correctly for $Z_2 > 70$ and energies per $\mu > 0.25$ MeV/μ. In the rare-earth region the ECPSSR results lie above the data at higher projectile energies and fall off below the data at lower energies.

INTRODUCTION

In the last several years, a clearer picture of M-shell ionization has been established due to more consistent experimental measurements and renewed theoretical effort. The ECPSSR calculations[1] have been extended recently[2] to M-shell ionization. The ECPSSR approach, which is based on the perturbed-stationary-state approximation, goes beyond first-Born-approximation theory, i.e., the plane-wave Born approximation (PWBA)[3] for direct ionization to the continuum (DI) and the Oppenheimer-Brinkman-Kramers (OBK) approximation of Nikolaev (OBKN)[4] for electron capture to the ion (EC). The ECPSSR theory includes the considerations due to energy loss, Coulomb deflection, and relativistic effects. Satisfactory agreement between the predictions of ECPSSR theory and the measured data has been found for M-shell ionization by H^+ and He^+ ions for selected targets.[5] Experimentally, the availability of relatively high-resolution Si(Li) detectors since the early 1970's has helped to improve the precision of M-shell ionization measurements.[5–16] Uncertainties in the data have been reduced by overcoming difficulties associated with the determination of the efficiency of the Si(Li) detector in the low-energy region of M-shell x rays (0.8—4 keV). In addition, the quality of the measurements has improved due to elimination of low-Z contaminant backgrounds, which have 1—4-keV K-shell x rays that overlap the M-shell x-rays' range. The literature for M-shell x-ray studies with $^1H^+$ and $^4He^+$ ions indicates a lack of experimental data especially in the rare-earth region. The primary difficulties associated with M-shell x-ray measurements for elements in the rare-earth region are related to the low energies of the M-shell x rays (0.8—1.6 keV). The uncertainties in the efficiency of the Si(Li) detector are large at these energies. For some of the rare-earth elements, low-Z contaminants come from the extraction process used in production of rare earths. For targets of $_{58}$Ce, $_{59}$Pr, and $_{60}$Nd, the $_{11}$Na and $_{12}$Mg contaminant K-shell x rays interfere with the M-shell x-ray spectrum. Silicon contamination produces K-shell x rays which overlap the M-shell x rays of $_{71}$Lu and $_{72}$Hf.

Over the years, the M-shell x-ray region for $Z_2 \geq 79$ has been studied in more detail than any other region. The ECPSSR predictions are in satisfactory agreement with the measured data in the 0.3—2.6-MeV range for both $^1H^+$ and $^4He^+$ ions.[5] Detailed studies are not available for lighter rare-earth targets. The work that is available has uncertainties greater than 15%. The recent interest in the rare-earth region is not only to fill in the gaps in the data, but also to investigate the nature of M-shell x-ray production with energy and the target atomic number Z_2. The ECPSSR theory predicts a maximum in M-shell x-ray-production cross section when plotted versus Z_2 in the

TABLE I. M-shell x-ray-production cross sections in barns by incident $^1_1H^+$ ions.

Target element	Effective thickness ($\mu g/cm^2$)	Proton energy (MeV) 0.25	0.5	0.75	1.0	1.25	1.5	1.75	2.0	2.25	2.5
$_{59}Pr$[a]	15.7	152	406	576	807	844	926	1005	1174	1214	1099
$_{60}Nd$	16.1	156	406	627	767	827	937	1172	1136	1225	
$_{63}Eu$[a]	17.7				619	753	901	1007	1057	1125	1061
$_{64}Gd$	14.8	230	424	646	795	922	1057	1170	1174	1283	
$_{66}Dy$[a]	13.6	241	430	641	837	1039	1201	1302	1384	1532	1591
$_{67}Ho$[a]	13.0	207	426	611	807	1034	1094	1247	1439	1606	
$_{68}Er$	9.7	245	456	590	817	940	1110	1474	1576	1741	
$_{70}Yb$[a]	14.7	216	455	670	858	1107	1307	1601	1703	1713	
$_{72}Hf$	11.4	236	493	728	929	1115	1375	1527	1511	1606	

[a]Actual energies were 0.20, 0.45, 0.70, 0.95, 1.21, 1.46, 1.71, 1.96, 2.22, and 2.47 MeV.

rare-earth region.[17]

In the present paper the M-shell x-ray-production cross sections are reported for thin targets ($\sim$10–20 $\mu g/cm^2$) of $_{59}Pr$, $_{60}Nd$, $_{63}Eu$, $_{64}Gd$, $_{66}Dy$, $_{67}Ho$, $_{68}Er$, $_{70}Yb$, and $_{72}Hf$ for incident $^1H^+$ and $^4He^+$ ions. The energies of these ions ranged from 0.25 to 2.5 MeV. The data are compared to the predictions of first Born approximation, i.e., the PWBA for DI, and the OBKN approximation for EC and the ECPSSR approximation. For the purpose of comparison, the M-shell ionization cross sections were converted to production cross sections using the single-hole fluorescence yields, Coster-Kronig transition rates, and branching ratios for each individual subshells.[18] In addition, a survey of M-shell x-ray-production cross-section measurements of elements in the range $Z_2=54$ to 92 is made for incident $^1H^+$ and $^4He^+$ ions. The data are compared to the predictions of the ECPSSR theory.

EXPERIMENTAL PROCEDURE AND DATA ANALYSIS

Ion beams of $^1H^+$ and $^4He^+$ were obtained from the 2.5-MV Van de Graaff accelerator at North Texas State University. Thin targets ($\sim$7–20 $\mu g/cm^2$) of $_{59}Pr$, $_{60}Nd$, $_{63}Eu$, $_{64}Gd$, $_{66}Dy$, $_{67}Ho$, $_{68}Er$, $_{70}Yb$, and $_{72}Hf$ were prepared by vacuum evaporation and deposition of the elements on thin ($\sim$15–20 $\mu g/cm^2$) carbon foils. Precautions were taken to assure nearly contaminant-free targets. These methods of pure target fabrication have been discussed elsewhere.[19] The elemental layers were thin enough to make energy loss of the incident ions minimal, but were thick enough so as to provide a clean spectrum above the background. Tables I and II list the measured average thicknesses.

The x rays and the scattered particles produced in the projectile-ion–target-atom interaction were measured by a Si(Li) detector and a Si surface-barrier detector, respectively. The scattering chamber geometry was such that the targets were positioned at 45° to the incident beam direction, while the Si(Li) and the particle detector were located at 90° and 150° to the beam, respectively. Details of the experimental setup, efficiency determination, and data analysis have been discussed elsewhere.[5] The primary uncertainties in the cross-section measurements come from (i) background subtraction and polynomial fitting and (ii) efficiency of the Si(Li) detector at the M x-ray energy. These two uncertainties contributed most for targets of $_{59}Pr$ and $_{60}Nd$. Typically, the background subtraction was uncertain by 5–10 % while efficiency was known to be within 5–15 %. The total absolute uncertainties in these cross-section measurements ranged from 10–25 % for the ion-target combinations studied here.

RESULTS, DISCUSSION, AND CONCLUSIONS

Among all the elements reported in the literature for M-shell x-ray production, gold and lead have been investigated with the greatest frequency. A plot of the M-shell

TABLE II. M-shell x-ray-production cross sections in barns by incident $^4_2He^+$ ions.

Target element	Effective thickness ($\mu g/cm^2$)	$^4_2He^+$ energy (MeV) 0.25	0.5	0.75	1.0	1.25	1.5	1.75	2.0	2.25	2.5
$_{59}Pr$[a]	15.7	122	232	474	750	1049	1333	1598	1871	2209	2520
$_{60}Nd$	16.1	83.7		589	813	1060	1361	1428	1626	1674	
$_{63}Eu$[a]	17.7	56.3	168	374	562	759	910	1228	1420	1647	1892
$_{64}Gd$	14.8	67.9	181	373	502	923	1063	1072	1424	1651	
$_{66}Dy$[a]	13.6	70.7	207	433	676	952	1189	1487	1760	1977	2311
$_{67}Ho$[a]	13.0	36.3	176	402	641	899	1194	1434	1742	2041	2345
$_{68}Er$	9.7	40.1	210	350	499	834	1050	1288	1150	1242	
$_{70}Yb$[a]	14.7	32.9	163	353	543	840	1049	1334	1572	2144	2494
$_{72}Hf$	11.4	45.9	164	335	513	967	1235	1170	1478	1554	

[a]Actual energies were 0.20, 0.45, 0.70, 0.95, 1.21, 1.46, 1.71, 1.96, 2.22, and 2.47 MeV.

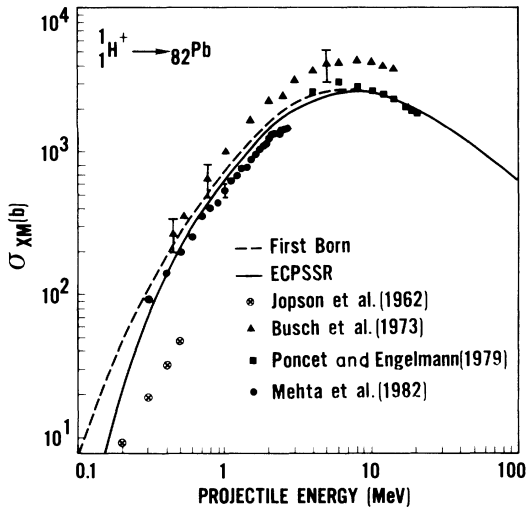

FIG. 1. M-shell x-ray-production cross sections for protons incident on lead vs incident projectile energy. Data from Refs. 5, 10, 14, and 20 are compared to the first-Born-approximation (PWBA plus OBKN) and ECPSSR theories.

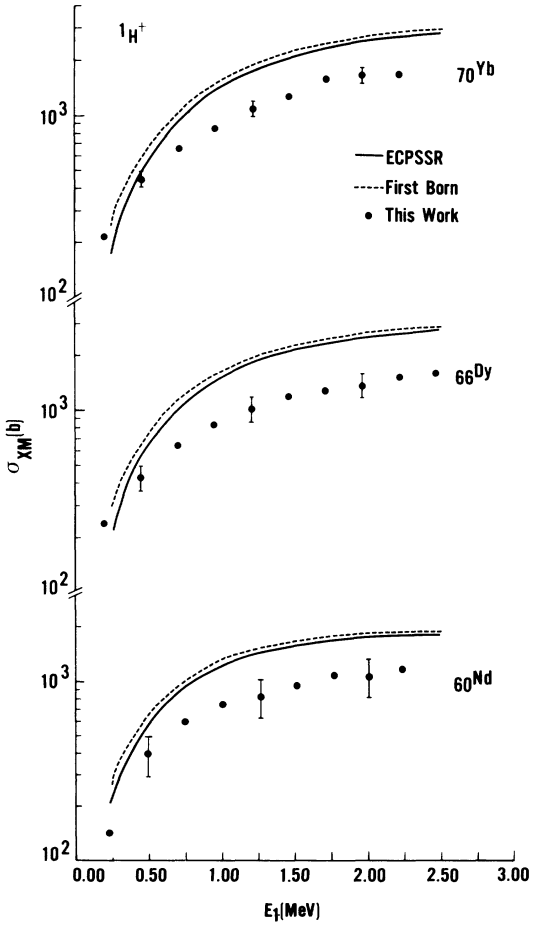

FIG. 2. M-shell x-ray-production cross sections for protons incident on neodymium, dysprosium, and ytterbium in the energy range from 0.25 to 2.5 MeV. Predictions of first-Born-approximation (dashed curve) and ECPSSR (solid curve) theories are shown.

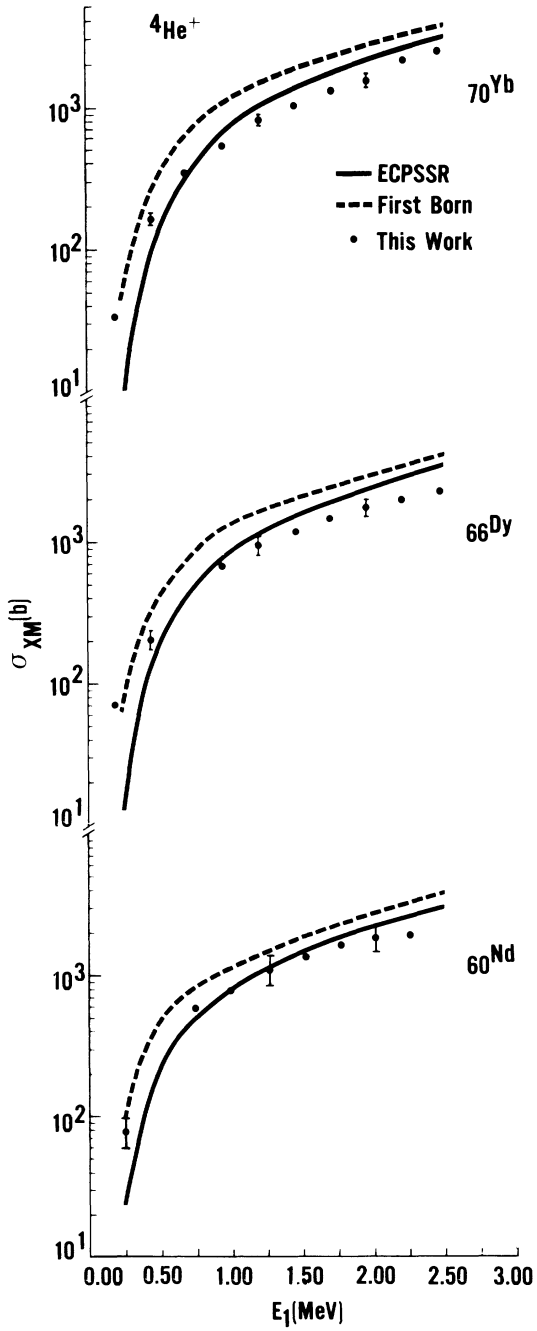

FIG. 3. M-shell x-ray-production cross section for singly ionized helium incident on neodymium, dysprosium, and ytterbium in the energy range from 0.25 to 2.5 MeV. Predictions of first-Born-approximation (dashed curve) and ECPSSR (solid curve) theories are shown.

x-ray-production cross sections for $_{82}Pb$ for incident $^1H^+$ ions is shown in Fig. 1 versus proton energy. Measurements performed at various laboratories are also shown on this graph. The data and all the theories shown on the curves are for x-ray-prodution cross sections. The predictions of the first-Born-approximation theories, i.e., the PWBA for DI plus the OBK approximation of Nikolaev

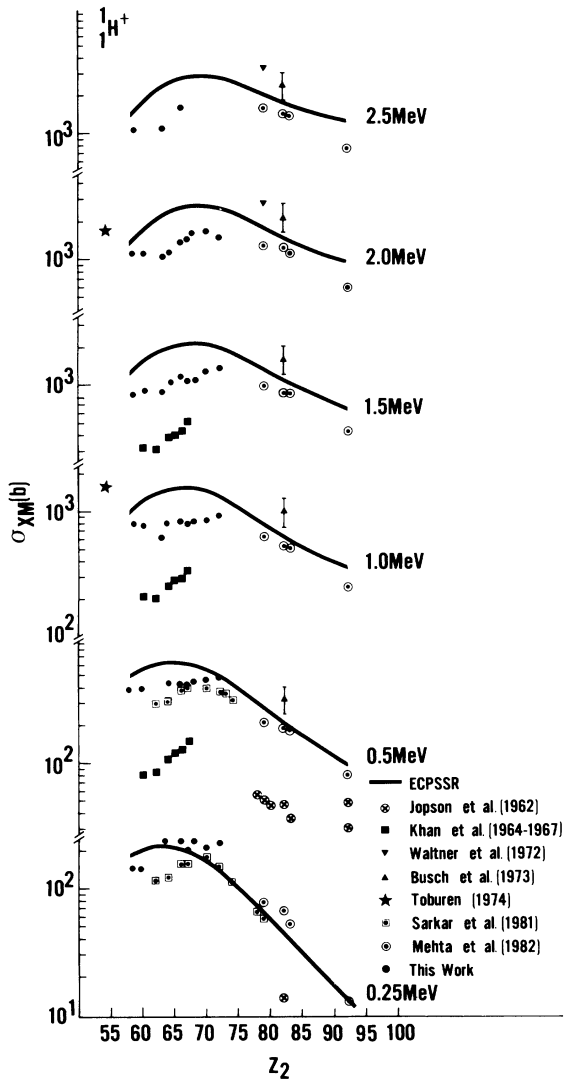

FIG. 4. M-shell x-ray-production cross sections for protons ranging in energy from 0.25 to 2.5 MeV, incident on various targets of atomic numbers $54 \leq Z_2 \leq 92$. Data, some of which are taken from Refs. 5, 9, 10, 16, 20, 22, and 23, are compared to the ECPSSR theory. At $60 \leq Z_2 \leq 70$, the data lie below the theory, while at $70 < Z_2 \leq 92$, the theory shows agreement with recent measurements.

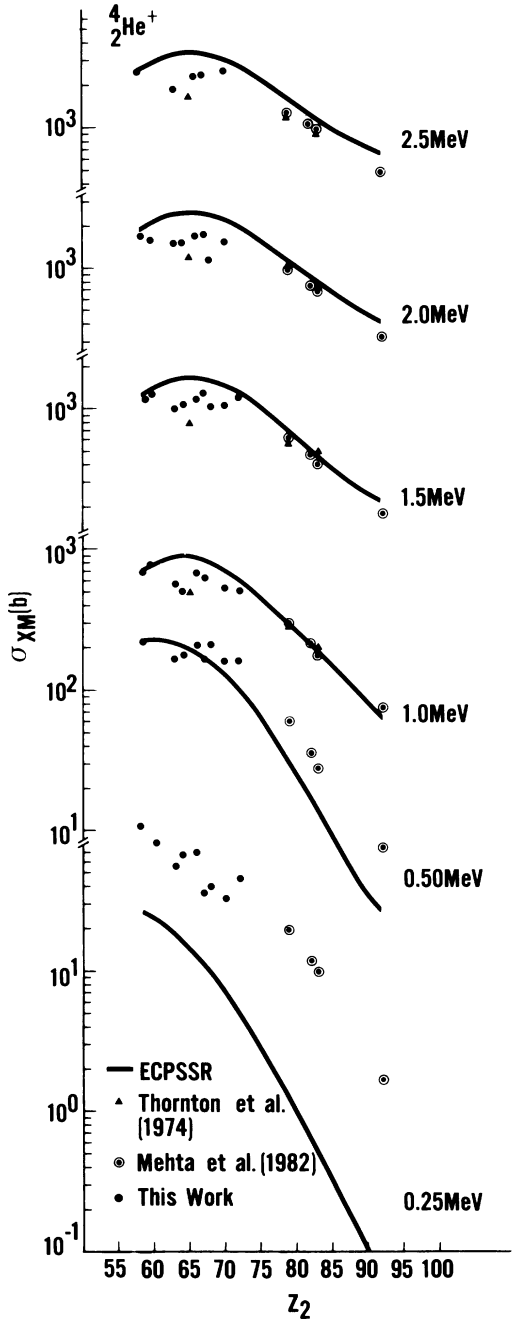

FIG. 5. M-shell x-ray-production cross sections for singly ionized helium, ranging in energy from 0.25 to 2.5 MeV, incident on various targets of atomic numbers $59 \leq Z_2 \leq 92$. Data, some of which are taken from Refs. 5 and 11, are compared to the ECPSSR theory. At lower energy, the theory lies below the data, while better agreement is obtained at higher energies.

for EC (dashed curve) and the ECPSSR (solid curve) theory were converted from M-shell ionization cross sections to production cross sections using the fluorescence yield, Coster-Kronig transition rates, and branching ratios for each of the subshells.[18] Electron capture contribution is negligible (estimated in the ECPSSR theory as 0.3%). Most of the data from various reported measurements are in fair agreement with each other. At low energies the exploratory work of Jopson *et al.*[20] is considerably lower than both the theoretical curve and other reported measurements.[5,10] In order to include the measurements of Poncet and Engelmann[14] on this curve, we have reconverted their ionization cross-section data to x-ray-production cross sections using the average M-shell fluorescence yield $\bar{\omega}_M$ of their choice.[21] The first-Born-approximation predictions lie higher than the ECPSSR theory for $^1_1H^+$ ions with energies below 7 MeV. Overall, the ECPSSR theory is in good agreement with the data. Figure 1 shows that present theories can predict these total cross sections in the 0.3—20-MeV range with sufficient accuracy. The recent measurements are in better agreement with theory than results obtained from experiments performed in the early 1960's and 1970's.

Figure 2 presents M-shell x-ray-production cross sections of $_{60}$Nd, $_{66}$Dy, and $_{70}$Yb for $^1_1H^+$ ions versus the ion energy. The predictions of the first-Born-approximation (dashed curve) and ECPSSR (solid curve) theories are also plotted. Both theories overpredict the data, increasingly so with the increasing energy. The first Born approximation overpredicts all of the data by large amounts. The ECPSSR curve is somewhat closer to the data points than the first Born approximation though it fails in the same way at high energies.

Figure 3 shows the M-shell x-ray-production cross section of $_{60}$Nd, $_{66}$Dy, and $_{70}$Yb for incident $^4_2He^+$ ions versus the ion energy. Again, the first Born approximation overpredicts all of the data. The ECPSSR theory is in good agreement with the data at $\sim$0.5 MeV, overpredicts at higher energies, and underpredicts below 0.5 MeV. For the same element, the overestimation of the data by the ECPSSR theory is smaller for $^4_2He^+$ data than the $^1_1H^+$ data at the same energy per unit mass. Tables I and II list all the cross sections measured in this work.

Figures 4 and 5 display the M-shell x-ray-production cross-section measurements made over the last 20 years at various laboratories for incident $^1_1H^+$ and $^4_2He^+$ ions, respectively. The data and the predictions of ECPSSR theory are plotted versus Z_2 for 0.25-, 0.5-, 1.0-, 1.5-, 2.0-, and 2.5-MeV incident ion energy. The atomic number of the targets included in the graphs range from $Z_2=54$ to 92. On both of these figures the ordinate is broken into parts to exhibit otherwise closely spaced data in the kilobarn range.

In Fig. 4, experimental data follow the trend shown by the ECPSSR theory (solid curve). The measurements done in the 1960's and early 1970's lie well below measurements repeated later. Both Jopson *et al.*[20] and Khan *et al.*[22] used thick targets, and the cross sections were calculated using target stopping power for the particular ion. This explains the large uncertainties in these data points. Excellent agreement is seen for target data with $Z_2>70$ for hydrogen ions. For $Z_2<70$, the measured data points fall below the theory. The ECPSSR cross section peaks at $Z_2\simeq65$ and falls off at higher target atomic numbers. The experimental data follow this trend although the maximum appears to be shifted toward $Z_2=70$. An overview shows that there are gaps in the data for $Z_2<60$, $70<Z_2<79$, and $83<Z_2<92$.

Figure 5 shows M-shell x-ray-production cross section by Thornton *et al.*,[11] Mehta *et al.*,[5] and the present work for incident $^4He^+$ ions. Again, the ECPSSR theory (solid curve) predicts a maximum in the cross section that flattens and shifts to higher Z_2 with increasing energy of the ion. The data follow this trend closely. The overall agreement between the data and the ECPSSR theory is better for $^4He^+$ than for incident protons (see Fig. 4). The data points for a target with $Z_2>78$ are in excellent agreement with ECPSSR theory at energies ≥1.0 MeV. The data are underestimated by a large amount at lower energies of 0.5 and 0.25 MeV.

In conclusion, the overall agreement of the ECPSSR theory with the measured data is somewhat better for ^{4}He ions than for the ^{1}H ions. Both the data and the theory show a broad maximum in the cross section as a function of Z_2. Beyond this maximum, the cross sections fall off more rapidly for helium ions than for protons. At lower ion energies, the rapid falling off of the cross sections is reproduced in shape but not absolute magnitude by the ECPSSR theory. The ECPSSR theory predicts the M-shell production cross section correctly for targets with $Z_2>70$ and energies ≥0.25 MeV/μ. In the rare-earth region the ECPSSR results lie above the data at higher projectile energies and fall off below the data at lower energies.

ACKNOWLEDGMENTS

This work is supported in part by the Robert A. Welch Foundation and the State of Texas Organized Research Fund.

[1]W. Brandt and G. Lapicki, Phys. Rev. A 23, 1717 (1981).
[2]G. Lapicki, Bull. Am. Phys. Soc. 26, 1310 (1981).
[3]D. E. Johnson, G. Basbas, and F. D. McDaniel, At. Data Nucl. Data Tables 24, 1 (1979).
[4]J. R. Oppenheimer, Phys. Rev. 31, 349 (1928); H. C. Brinkman and H. A. Kramers, Proc. Acad. Sci. (Amsterdam) 33, 973 (1930); V. S. Nikolaev, Zh. Eksp. Teor. Fiz. 51, 1263 (1966) [Sov. Phys.—JETP 24, 847 (1967)].
[5]R. Mehta, J. L. Duggan, J. L. Price, F. D. McDaniel, and G. Lapicki, Phys. Rev. A 26, 1883 (1982).
[6]P. B. Needham, Jr. and B. D. Sartwell, Phys. Rev. A 2, 27 (1970); 2, 1686 (1971).
[7]P. H. Mokler, Phys. Rev. Lett. 26, 811 (1971).
[8]P. H. Mokler, H. J. Stein, and P. Armbruster, Phys. Rev. Lett. 29, 827 (1972).
[9]A. W. Waltner, D. M. Peterson, G. A. Bissinger, A. B. Baskins, C. E. Busch, P. H. Nettles, W. R. Scates, and S. M. Shafroth, in *Proceedings of the International Conference on Inner Shell Ionization Phenomena and Future Applications, Atlanta, Georgia, 1972,* edited by R. W. Fink, S. T. Manson, J. M. Palms, and P. V. Rao (U.S. AEC, Oak Ridge, Tenn., 1973), p. 1080.
[10]C. E. Busch, A. B. Baskin, P. H. Nettles, S. M. Shafroth, and A. W. Waltner, Phys. Rev. A 7, 1601 (1973).
[11]S. T. Thornton, R. H. McKnight, and R. R. Karlowicz, Phys. Rev. A 10, 219 (1974).
[12]K. Ishii, S. Morita, H. Tawara, H. Kaji, and T. Shiokawa, Phys. Rev. A 11, 219 (1975).
[13]V. S. Nikolaev, V. P. Petukhov, E. A. Romanovsky, V. A. Sergeev, I. M. Kruglova, and V. V. Beloshitsky, *The Physics of Electronic and Atomic Collisions* (University of Washington Press, Seattle, 1975), p. 419.
[14]M. Poncet and C. Engelmann, Nucl. Instrum. Methods 159, 455 (1979).
[15]K. Sera, K. Ishii, A. Yamadera, A. Kuwako, M. Kamiya, M. Sebata, S. Morita, and T. C. Chu, Phys. Rev. A 22, 2536 (1980).
[16]M. Sarkar, H. Mommsen, W. Sarter, and P. Schurkes, J. Phys. B 14, 3163 (1981).

[17]R. Mehta, J. L. Duggan, F. D. McDaniel, P. M. Kocur, J. L. Price, and G. Lapicki, IEEE Trans. Nucl. Sci. NS-30, 950 (1983).

[18]E. J. McGuire, Phys. Rev. A 5, 1043 (1972).

[19]P. M. Kocur, J. L. Duggan, R. Mehta, J. Robbins, and F. D. McDaniel, IEEE Trans. Nucl. Sci. NS-30, 1580 (1983).

[20]R. C. Jopson, H. Mark, and C. D. Swift, Phys. Rev. 127, A1612 (1962); R. C. Jopson, H. Mark, C. D. Swift, and M. A. Williamson, *ibid.* 137, A1353 (1965).

[21]W. Bambynek, B. Craseman, R. W. Fink, H.-U. Freund, H. Mark, C. D. Swift, R. E. Price, and P. V. Rao, Rev. Mod. Phys. 44, 716 (1972).

[22]J. M. Khan, D. L. Potter, and R. D. Worley, Phys. Rev. 135, A511 (1964); 136, A108 (1964); 145, 23 (1966); 163, 81 (1967).

[23]L. H. Toburen, Phys. Rev. A 9, 2505 (1974).